This article can be cited as S. Vrkalovic, E.-C. Lunca and I.-D. Borlea, Model-Free Sliding Mode and Fuzzy Controllers for Reverse Osmosis Desalination Plants, International Journal of Artificial Intelligence, vol. 16, no. 2, pp. 208-222, 2018.

Model-Free Sliding Mode and Fuzzy Controllers for Reverse Osmosis Desalination Plants

Sasa Vrkalovic[1], Elena-Cristina Lunca[2], Ioan-Daniel Borlea[2]

[1]Faculty of Electrical Engineering, University of East Sarajevo,

Bosnia and Herzegovina

sasa.vrkalovic@yahoo.com

[2]Dept. of Automation and Applied Informatics, Politehnica University of Timisoara,

Bd. V. Parvan 2, 300223 Timisoara, Romania

luncaelenacristina@yahoo.com, idborlea@gmail.com

ABSTRACT

This paper presents model-free sliding mode controllers and Takagi-Sugeno fuzzy controllers for the flux and conductivity control of Reverse Osmosis Desalination Plants (RODPs). The RODPs are Multi Input-Multi Output processes and two separate controllers are designed in Single Input-Single Output control systems. The design of the model-free sliding mode controllers is done by Lyapunov's stability theory. The Takagi-Sugeno fuzzy controllers are designed by considering linear matrix inequalities as constraints in an optimization problem solved by a Grey Wolf Optimizer algorithm. Simulation results are included.

Keywords: fuzzy control, Grey Wolf Optimizer algorithm, linear matrix inequalities, model-free sliding mode control, reverse osmosis desalination plants, stability.

Mathematics Subject Classification: 82C21, 93A30, 37N35, 34H10, 03E72, 34A34

Computing Classification System: I.2.3, I.2.8, I.2.9

1. INTRODUCTION

Reverse Osmosis Desalination Plants (RODPs) are important in the context of solving the water crisis problem in order to give fresh water of good quality and quantity. From a systemic point of view RODPs are nonlinear Multi Input-Multi Output (MIMO) processes (Gambier et al., 2007), and both the flux and the conductivity control must be done. Some of the important examples of modeling and control systems and algorithms for RODPs are: multi-objective optimization applied to tune the Proportional-Integral (PI) controllers in two Single Input-Single Output (SISO) control systems for separate flux and conductivity control (Gambier et al., 2009), the combination of an operational model for spiral-wound reverse osmosis desalting and a supervisory controller to provide real-time updates of membrane permeability (Gao et al., 2014), the optimal tuning of Proportional-Integral-Derivative (PID) controllers using Particle Swarm Optimization (PSO) (Rathore et al., 2013), teacher-learner-based-optimization (Rathore et al., 2018a), Grey Wolf Optimizer (GWO) (Rathore et al., 2018b), two-dimensional genetic algorithm (Lee et al., 2016) and robust control (Phuc et al., 2017).

Model-free sliding mode control has been proposed in (Precup et al., 2014) to combine the advantages of two control strategies, model-free data-driven control and sliding mode control. Some recent results on model-free sliding mode control are: sliding mode control is combined with a model-free intelligent PI (iPI) controller in (Precup et al., 2014) and applied to real-time servo system control; a mixed sliding mode control-model-free iPD controller is proposed in (Wang et al., 2015) and applied to a quadrotor system; sliding mode control combined with model-free adaptive control applied to a robotic exoskeleton is suggested in (Wang et al., 2016); two iPI-based model-free sliding mode control approaches are proposed in (Precup et al., 2017c) and applied to twin rotor aerodynamic systems, with the first one developed from (Precup et al., 2014) and the second one also applied in (Wang et al., 2017) but in an iPID formulation to an exosekeleton system; the first approach in (Precup et al., 2017c) is applied in (Khooban, 2018) to load frequency control in microgrids.

As shown in (Vrkalovic et al., 2017), stability is one of the most important problems in the analysis and design of nonlinear control systems. The stability issues related to fuzzy control systems have been studied seriously in the recent years, with examples presented in (Chang et al., 2017), (Du et al., 2017), (Haidegger et al., 2012), (Li et al., 2018), (Pozna et al., 2012), (Preitl et al., 2006), (Rathinasamy et al., 2018), (Škrjanc et al., 2002) and (Tomescu et al., 2007).

The optimal tuning of fuzzy controllers can guarantee systematic performance specifications in the conditions of model-based tuning. An overview on swarm intelligence algorithms applied to fuzzy controllers is given in (Precup et al., 2015). A part of the application of these algorithms includes Ant Colony Optimization (Castillo et al., 2015), chemical optimization (Melin et al., 2013), genetic algorithms (Das et al., 2013), (Perez et al., 2013), Simulated Annealing (Vrkalovic et al., 2017), PSO (Vrkalovic et al., 2017), Gravitational Search Algorithm (GSA) (Vrkalovic et al., 2017), harmony search (Wang et al., 2013) and GWO (Precup et al., 2017a), (Precup et al., 2017b). But the proper adaptation of other algorithms can also be considered (Kazakov and Lempert, 2015), (Purcaru et al., 2013).

This paper proposes two approaches to the control of RODPs. Both approaches use two SISO control systems for separate flux and conductivity control with appropriate controllers designed and tuned

after the application of decoupling. One of the approach is model-free sliding mode control as an application of the approach proposed in (Precup et al., 2014) with the design steps given in (Precup et al., 2017c), and the other approach is model-based fuzzy control. The model-based control is applied, as in (Vrkalovic et al., 2017), as a combination of swarm intelligence algorithms and stability by the optimal tuning of the parameters of Takagi-Sugeno fuzzy controllers using stability conditions expressed as linear matrix inequalities (LMIs) that are used as constraints in optimization problems. But this time a PI fuzzy controller expressed in state-space form is used, and the swarm intelligence algorithm is GWO.

The rest of the paper is structured as follows: Section 2 is dedicated to the modeling of RODPs and decoupling in the context of MIMO reduction to SISO. The steps of the model-free sliding mode approach are given in Section 3. The Takagi-Sugeno fuzzy control system models and stability analysis are treated in Section 4. The optimal tuning of fuzzy controllers is presented in Section 5. Section 6 offers simulation results, and conclusions are highlighted in Section 7.

2. MODELS OF REVERSE OSMOSIS DESALINATION PLANTS

The transfer function matrix of RODP is expressed as follows using the data taken from (Alatiqi et al., 1989), (Chaaben et al., 2011), (Riverol, C., Pilipovik, V., 2005), (Robertson et al., 1996):

$$\mathbf{G}(s)=\begin{bmatrix} G_{11}(s) & G_{12}(s) \\ G_{21}(s) & G_{22}(s) \end{bmatrix} \tag{1}$$

where the individual transfer functions between the two control inputs (pH $u_1 = A_s$ and feed pressure $u_2 = \theta_r$) and two controlled outputs (permeate water flux $y_1 = F_s$ and salinity or conductivity $y_2 = C_s$) in zero initial conditions are:

$$\begin{aligned} &G_{11}(s)=\frac{F_s}{A_s}=\frac{k_{11}}{1+T_{11}s}, G_{12}(s)=\frac{F_s}{\theta_r}=\frac{-\omega_1^2}{s^2+2\xi_1\omega_1 s+\omega_1^2}, \\ &G_{21}(s)=\frac{C_s}{A_s}=\frac{-\omega_2^2}{s^2+2\xi_2\omega_2 s+\omega_2^2}, G_{22}(s)=\frac{C_s}{\theta_r}=\frac{k_{22}}{1+T_{22}s} \end{aligned} \tag{2}$$

where the values of model parameters obtained at salinity or disturbance $C_f = 3000\,\mu\text{S/cm}$ are (Chaaben et al., 2011):

$$k_{11}=3, T_{11}=T_{22}=1.1\,\text{s}, k_{22}=-0.16, \omega_1=1.2\,\text{s}^{-1}, \omega_2=1.72\,\text{s}^{-1}, \xi_1=0.3, \xi_2=0.45 \tag{3}$$

The MIMO control system structure is presented in Figure 1. This structure points out the flux controller C_1, the conductivity controller C_2, the two SISO control loops with the water flux reference input r_1 and control error e_1, and the conductivity reference input r_2 and control error e_2.

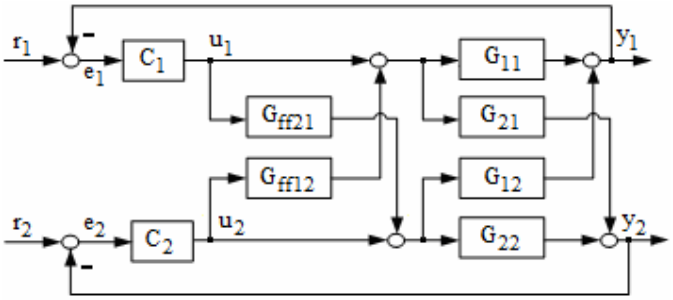

Figure 1. MIMO control system structure for RODP.

Since the two control loops interact, the decoupling is done for a relatively simple controller design. This is done in terms of adding the feedforward decoupler blocks with the transfer functions $G_{ff12}(s)$ and $G_{ff21}(s)$ in Figure 1. The actuators and measurement blocks dynamics are included in the model and parameters (1) to (3) and the two control signals keep the same notation for the sake of simplicity. The transfer function matrix of the process plus decoupler is:

$$\begin{aligned}\mathbf{G}_P(s) &= \mathbf{G}(s)\cdot\begin{bmatrix}1 & G_{ff12}(s)\\ G_{ff21}(s) & 1\end{bmatrix}\\ &=\begin{bmatrix}G_{11}(s)+G_{12}(s)G_{ff21}(s) & G_{11}(s)G_{ff12}(s)+G_{12}(s)\\ G_{21}(s)+G_{22}(s)G_{ff21}(s) & G_{21}(s)G_{ff12}(s)+G_{22}(s)\end{bmatrix}\end{aligned} \tag{4}$$

Imposing zero elements on the antidiagonal of the matrix $\mathbf{G}_P(s)$ to ensure ideal decoupling, the decoupler is computed as:

$$G_{ff12}(s)=-\frac{G_{12}(s)}{G_{11}(s)}, G_{ff21}(s)=-\frac{G_{21}(s)}{G_{22}(s)} \tag{5}$$

Therefore, the decoupled process is represented by the transfer function matrix:

$$\begin{aligned}\mathbf{G}_P(s) &= \begin{bmatrix}P_{11}(s) & 0\\ 0 & P_{22}(s)\end{bmatrix}\\ &=\begin{bmatrix}\dfrac{G_{11}(s)G_{22}(s)-G_{12}(s)G_{21}(s)}{G_{22}(s)} & 0\\ 0 & \dfrac{G_{11}(s)G_{22}(s)-G_{12}(s)G_{21}(s)}{G_{11}(s)})\end{bmatrix}\end{aligned} \tag{6}$$

where $P_{11}(s)$ is the decoupled process transfer function for flux control and $P_{22}(s)$ is the decoupled process transfer function for conductivity or salinity control.

The detailed expressions of $P_{11}(s)$ and $P_{22}(s)$ are not presented here. However Preitl and Precup's Extended Symmetrical Optimum method can be applied to such processes due to its robustness feature (Precup et al., 2009), (Precup et al., 2013), (Vrkalovic, 2015).

3. MODEL-FREE SLIDING MODE CONTROL DESIGN

The model-free sliding mode control system structure for one of the two control loops is presented in Figure 2, therefore the subscripts 1 and 2 are eliminated as follows, and its design approach consists of the following steps (Precup et al., 2017c):

- Step 1. Set the design parameter $\alpha > 0$ such that $\dot{y}(t)$ and $\alpha\, u(t)$ should have the same order of magnitude, where the first order local process model used for controlling $P_{11}(s)$ or $P_{22}(s)$ is:

$$\dot{y}(t) = F(t) + \alpha\, u(t) \tag{7}$$

- Step 2. Choose the parameters of the first order derivative plus low-pass filter with the transfer function:

$$H_{Lp1}(s) = \frac{K_{Lp1} s}{1 + T_{Lp1} s} \tag{8}$$

such that to ensure a tradeoff to noise reduction and delay induced by the filter.

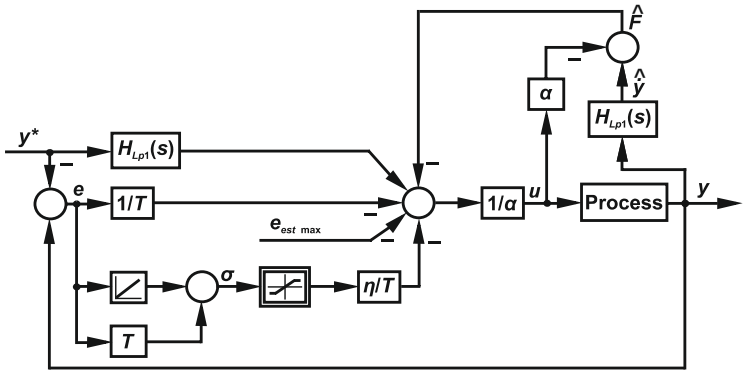

Figure 2. Model-free sliding mode control system structure (Precup et al., 2017c) applied to both control loops presented in Figure 1.

- Step 3. Estimate a small value for the design parameter $e_{est\max}$, where $e_{est}(t)$ is the estimation error of $F(t)$:

$$e_{est}(t) = \dot{e}(t) + K_P\, e(t) + K_I \int_0^t e(\tau) d\tau \tag{9}$$

$|e_{est}(t)| \le e_{est\max}$, and K_P and K_I are the proportional and integral gains of the PI controller in the structure of iPI controller, but they do not affect the design.

- Step 4. Set the design parameter $T > 0$ to prescribe the desired behavior of the control system on the sliding manifold, where the switching variable is $\sigma(t)$:

$$\sigma(t) = x_1(t) + T\, x_2(t), x_1(t) = \int_0^t e(\tau)d\tau, x_2(t) = e(t) \tag{10}$$

and the expression of the nonlinear block specific to the boundary layer approach in Figure 1 is:

$$\text{sat}(\sigma(t), \varepsilon) = \begin{cases} -1 & \text{if } \sigma(t) < -\varepsilon \\ \dfrac{\sigma(t)}{\varepsilon} & \text{if } |\sigma(t)| \le \varepsilon \\ 1 & \text{if } \sigma(t) > \varepsilon \end{cases} \tag{11}$$

where $\eta > 0$ and $\varepsilon > 0$ are the convergence factor and the boundary layer thickness, respectively.

- Step 5. Set the parameters $\eta > 0$ and $\varepsilon > 0$ using inequalities (Precup et al., 2017c):

$$|\sigma(t)|\,\eta > 2T\, e_{est\max}, + T\,[e_{est\infty} - e_{est\max}] - \frac{\eta\,\sigma_\infty}{\varepsilon} = 0 \tag{12}$$

where $e_{est\infty}$ is the steady-state estimation error.

4. FUZZY CONTROL SYSTEM MODELS AND STABILITY ANALYSIS

The presentation will be given again for one of the two control loops in Figure 1, where C_1 and C_2 are Takagi-Sugeno PI-fuzzy controllers, and the subscripts 1 and 2 will be omitted as follows. Since the process model presented in (6) is a simplified one and the decoupling cannot be perfect in practice, the process model that depend on the parameters in (3) are nominal ones, and they can be subjected to variations and parametric uncertainties. Some models and the stability analysis results are taken from (Vrkalovic et al., 2017), but with bold notations for matrices and vectors. The i^{th} rule of the fuzzy model for process with parametric uncertainties is:

$$\begin{aligned} &\text{Rule } i\text{: IF } z_1(t) \text{ IS } M_{ij} \text{ AND} \ldots \text{AND } z_p(t) \text{ IS } M_{ip} \\ &\text{THEN} \begin{cases} \dot{\mathbf{x}}(t) = (\mathbf{A}_i + \Delta\mathbf{A}_i)\mathbf{x}(t) + (\mathbf{B}_i + \Delta\mathbf{B}_i)\mathbf{u}(t) \\ \mathbf{y}(t) = \mathbf{C}_i\mathbf{x}(t) \end{cases} \end{aligned} \tag{13}$$

where M_{ij} is a fuzzy set (linguistic term), $\mathbf{x}(t) \in R^n$ is the system state vector, $\mathbf{u}(t) \in R^m$ is the control signal vector, $m = 1$ as follows for a SISO control loop, so the notation $\mathbf{u}(t) = u(t)$ will also be

used, $\mathbf{y}(t) \in R^p$ is the process output and for the same reason $p = 1$ and $\mathbf{y}(t) = y(t)$, $\mathbf{A}_i, \mathbf{B}_i, \mathbf{C}_i$ are known constant matrices that describe the nominal process, and $z_1(t), z_2(t), ..., z_p(t)$ are the premise (scheduling) variables, which belong to the input or scheduling vector $\mathbf{z}(t) = [z_1(t)\ z_2(t) \dots z_p(t)]^T$, $i = 1 \dots n_R$ and n_R is the number of rules.

The matrices $\Delta\mathbf{A}_i, \Delta\mathbf{B}_i$ in (13) are parametric uncertainties of the process, and have the following bounded structure:

$$\left[\Delta\mathbf{A}_i(t), \Delta\mathbf{B}_i(t)\right] = \mathbf{H}_i\mathbf{F}_i(t)\left[\mathbf{E}_{1i}, \mathbf{E}_{2i}\right], i = 1 \dots n_R, \mathbf{F}_i^T(t)\mathbf{F}_i(t) \le \mathbf{I} \tag{14}$$

where $\mathbf{H}_i, \mathbf{E}_{1i}, \mathbf{E}_{2i}$ are known real constant matrices, $\mathbf{F}_i(t)$ is an unknown matrix function with Lebesgue-measurable element, and $\mathbf{I}$ is the identity matrix.

The inputs of the Takagi-Sugeno PI-fuzzy controller (both input and premise variables) are the control error $e(t)$ and the integral of control error $e_I(t)$ obtained as the state variable of the integral part of the linear PI controller, which is actually fuzzified:

$$e_I(t) = \int_0^t e(\tau)d\tau \tag{15}$$

The computation of the derivative of both terms in (15) using the expression of the control error and (15) leads to the dynamics of the integral part of the linear PI controller:

$$\dot{e}_I(t) = r(t) - \mathbf{C}_i\mathbf{x}(t), i = 1 \dots n_R \tag{16}$$

Considering three linguistic terms for $e(t)$ and three linguistic terms for $e_I(t)$, the expression of i^{th} rule in the rule base of the Takagi-Sugeno PI-fuzzy controller is ($n_R = 9$ for Parallel Distributed compensation (PDC)):

$$\begin{aligned} &\text{Rule } i\text{: IF } e(t) \text{ IS } \text{LT}_{i1} \text{ AND } e_I(t) \text{ IS } \text{LT}_{i2} \\ &\text{THEN } u^i(t) = k_C^i e(t) + (k_C^i / T_i^i)e_I(t), i = 1 \dots n_R \end{aligned} \tag{17}$$

where $u^i(t)$ are the local control signals, k_C^i are the gains and T_i^i are the integral time constants.

Using the PROD operator to model the AND function in the rule antecedent, each fuzzy rule generates a firing degree $\mu_i, 0 \le \mu_i \le 1$ (of i^{th} rule) according to:

$$\mu_i = \prod_{i=1}^{n} M_{ij} z(t), h_i = (z(t)) = \frac{\mu_i(z(t))}{\sum_{i=1}^{r} \mu_i(z(t))} \tag{18}$$

where h_i is the normalized firing degree. The condition (18) written for the process corresponds to the following condition for the controller:

$$\mu_i(t) = \mu_{LTi1}(e(t))\mu_{LTi2}(e_I(t)), i = 1...n_R \tag{19}$$

The weighted average defuzzification method produces the output of the Takagi-Sugeno PI-fuzzy controller represented by the control signal $u(t)$:

$$u(t) = \frac{\sum_{i=1}^{n_R} \alpha_k(t) u^k(t)}{\sum_{i=1}^{n_R} \alpha_k(t)} = \sum_{i=1}^{n_R} h_i(t) u^i(t) = \sum_{i=1}^{n_R} h_i(t)(k_C^i e(t) + (k_C^i / T_i^i) e_I(t)) \tag{20}$$

Using the definition of $e(t)$ and the substition of the second equation taken from the state-space model in the rule consequent (in (13)) in (20), the expression of the control signal $u(t)$ is:

$$u(t) = -\sum_{i=1}^{n_R} h_i(t) k_C^i \mathbf{C}_i \mathbf{x}(t) + \sum_{i=1}^{n_R} h_i(t)(k_C^i / T_i^i) e_I(t) + \sum_{i=1}^{n_R} h_i(t) k_C^i r(t) \tag{21}$$

The Takagi-Sugeno fuzzy model of the process with parametric uncertainties is:

$$\begin{aligned} \dot{\mathbf{x}}(t) &= \sum_{i=1}^{n_R} h_i(\mathbf{z}(t))((\mathbf{A}_i + \Delta\mathbf{A}_i)\mathbf{x}(t) + (\mathbf{B}_i + \Delta\mathbf{B}_i)\mathbf{u}(t)) \\ \mathbf{y}(t) &= \sum_{i=1}^{n_R} h_i(\mathbf{z}(t))\mathbf{C}_i \mathbf{x}(t) \end{aligned} \tag{22}$$

where $h_i(\mathbf{z}(t)) \geq 0$, $i = 1...n_R$, and $\sum_{i=1}^{n_R} h_i(\mathbf{z}(t)) > 0$. Finally, the substitution of $\mathbf{u}(t) = u(t)$ from (21) in (22) leads to the state-space model of the fuzzy control system with parametric uncertainties. Introducing the augmented state vector $\bar{\mathbf{x}}(t)$:

$$\bar{\mathbf{x}}(t) = [\mathbf{x}^T(t) \quad e_I(t)]^T \tag{24}$$

the Takagi-Sugeno PI-fuzzy controller can be expressed as the following state feedback form specific to PDC:

$$\text{IF } z_1(t) \text{ IS } M_{ij} \text{ AND} ... \text{ AND } z_p(t) \text{ IS } M_{ip} \text{ THEN } u(t) = -\mathbf{k}_i \bar{\mathbf{x}}(t) \tag{25}$$

where $\mathbf{k}_i = [k_{i\omega\eta}]_{\omega=1...n+1, \eta=1...m} \in R^{(n+1)\times m}$ are constant state feedback gain matrices, which are expressed from (21) and (23):

$$\mathbf{k}_i = [\mathbf{C}_i \quad (k_C^i / T_i^i)] \tag{26}$$

The gain matrices $\mathbf{k}_i$ will be computed using GWO.

The modified expression of (13) with the augmented system matrices is:

$$\begin{aligned}
&\text{Rule}\, i:\ \text{IF}\, z_1(t)\,\text{IS}\, M_{ij}\ \text{AND}\ldots\text{AND}\, z_p(t)\,\text{IS}\, M_{ip}\\
&\text{THEN}\begin{cases}\dot{\overline{\mathbf{x}}}(t) = (\overline{\mathbf{A}}_i + \Delta\overline{\mathbf{A}}_i)\overline{\mathbf{x}}(t) + (\overline{\mathbf{B}}_i + \Delta\overline{\mathbf{B}}_i)\mathbf{u}(t) + \mathbf{B}_r r(t)\\ \mathbf{y}(t) = \overline{\mathbf{C}}_i\overline{\mathbf{x}}(t)\end{cases}\\
&\overline{\mathbf{A}}_i = \begin{bmatrix}\mathbf{A}_i & \mathbf{0}\\ -\mathbf{C}_i & 0\end{bmatrix}, \overline{\mathbf{B}}_i = \begin{bmatrix}\mathbf{B}_i\\ 0\end{bmatrix}, \overline{\mathbf{C}}_i = [\mathbf{C}_i \quad 0], \mathbf{B}_r = \begin{bmatrix}\mathbf{0}\\ 1\end{bmatrix}
\end{aligned} \tag{27}$$

where $\mathbf{B}_r r(t)$ is a disturbance term in the context of stability analysis.

The combination of (25) and (27) leads to the state-space model of the Takagi-Sugeno fuzzy control system with parametric uncertainties:

$$\begin{aligned}
\dot{\overline{\mathbf{x}}}(t) &= \sum_{i=1}^{n_R} h_i(\mathbf{z}(t)) \sum_{j=1}^{n_R} h_j(\mathbf{z}(t))[(\overline{\mathbf{A}}_i + \Delta\overline{\mathbf{A}}_i) - (\overline{\mathbf{B}}_i + \Delta\overline{\mathbf{B}}_i)\mathbf{k}_j]\overline{\mathbf{x}}(t) + \sum_{i=1}^{n_R} h_i(\mathbf{z}(t)) \sum_{j=1}^{n_R} h_j(\mathbf{z}(t))\mathbf{B}_r r(t)\\
\mathbf{y}(t) &= \sum_{i=1}^{n_R} h_i(\mathbf{z}(t))\overline{\mathbf{C}}_i\overline{\mathbf{x}}(t)
\end{aligned} \tag{28}$$

The main results on the stable design of the Takagi-Sugeno fuzzy control system with parametric uncertainties are expressed as the following theorem:

Theorem 1. The Takagi-Sugeno fuzzy system modeled in (28) is globally asymptotically stable if there exists a symmetric and positive definite matrix $\mathbf{P}$ and some scalar β that fulfill the following two sets of LMIs:

$$\begin{bmatrix}\mathbf{P}\,\overline{\mathbf{A}}_i + \overline{\mathbf{A}}_i^T\mathbf{P} - \mathbf{P}\,\overline{\mathbf{B}}_i\mathbf{k}_i - \mathbf{k}_i^T\overline{\mathbf{B}}_i^T\mathbf{P} & \mathbf{E}_{1i} - \mathbf{E}_{2i}\mathbf{k}_i & \mathbf{P}\,\mathbf{H}_i^T\\ * & -\beta^{-1}\mathbf{I} & 0\\ * & * & -\beta\mathbf{I}\end{bmatrix} < 0, i = 1\ldots n_R \tag{29}$$

$$\begin{bmatrix}\mathbf{P}\,\overline{\mathbf{A}}_i + \overline{\mathbf{A}}_i^T\mathbf{P} + \mathbf{P}\,\overline{\mathbf{A}}_j + \overline{\mathbf{A}}_j^T\mathbf{P} - \mathbf{P}\,\overline{\mathbf{B}}_i\mathbf{k}_j - \mathbf{k}_j^T\overline{\mathbf{B}}_i^T\mathbf{P} - \mathbf{P}\,\overline{\mathbf{B}}_j\mathbf{k}_i - \mathbf{k}_i^T\overline{\mathbf{B}}_j^T\mathbf{P} & \mathbf{E}_{1i} - \mathbf{E}_{2i}\mathbf{k}_j & \mathbf{E}_{1j} - \mathbf{E}_{2j}\mathbf{k}_i & \mathbf{P}\,\mathbf{H}_i^T & \mathbf{P}\,\mathbf{H}_j^T\\ * & -\beta^{-1}\mathbf{I} & 0 & 0 & 0\\ * & * & -\beta^{-1}\mathbf{I} & 0 & 0\\ * & * & * & -\beta\mathbf{I} & 0\\ * & * & * & * & -\beta\mathbf{I}\end{bmatrix} < 0, \tag{30}$$

$i, j = 1\ldots n_R, i < j$

Proof. This theorem is the generalization of Theorem 1 proposed in (Vrkalovic et al., 2017) to the augmented state-space system model. The sufficient conditions (29) and (30) that guarantee the

global asymptotic stability of the Takagi-Sugeno fuzzy control system with parametric uncertainties are derived as follows using Lyapunov-Krasovskii's method.

Let us consider the Lyapunov function V that is defined and fulfils:

$$V(\overline{\mathbf{x}}(t)) = \overline{\mathbf{x}}^T(t)\mathbf{P}\,\overline{\mathbf{x}}(t) > 0 \tag{31}$$

since $\mathbf{P} = \mathbf{P}^T > 0$. The derivative of the function in (31) is:

$$\dot{V}(\overline{\mathbf{x}}(t)) = 2\overline{\mathbf{x}}^T(t)\mathbf{P}\,\dot{\overline{\mathbf{x}}}(t) = \overline{\mathbf{x}}^T(t)\mathbf{P}\,\dot{\overline{\mathbf{x}}}(t) + \dot{\overline{\mathbf{x}}}^T(t)\mathbf{P}\,\overline{\mathbf{x}}(t) \tag{32}$$

Applying Lyapunov-Krasovskii's method to (32) using (28) leads to:

$$\mathbf{P}[\mathbf{A}_a + \mathbf{H}_a\mathbf{F}_a\mathbf{E}_a] + [\mathbf{A}_a^T + \mathbf{E}_a^T\mathbf{F}_a^T\mathbf{H}_a^T]\mathbf{P} < 0 \tag{33}$$

with the notations:

$$\mathbf{A}_a = \overline{\mathbf{A}}_i - \overline{\mathbf{B}}_i\mathbf{k}_j, \mathbf{E}_a = \mathbf{E}_{1i} - \mathbf{E}_{2i}\mathbf{k}_j, \mathbf{H}_a = \mathbf{H}_i, \mathbf{F}_a = \mathbf{F}_i \tag{34}$$

and appropriate dimensions. Equation (33) is next written as:

$$\varphi + \mathbf{R}\,\mathbf{F}_a\mathbf{E}_a + \mathbf{E}_a^T\mathbf{F}_a^T\mathbf{R}^T < 0 \tag{35}$$

with the notations:

$$\varphi = \mathbf{P}\,\mathbf{A}_a + \mathbf{A}_a^T\mathbf{P}, \mathbf{R} = \mathbf{P}\,\mathbf{H}_a \tag{36}$$

and (16) leads to:

$$\mathbf{R}^T = \mathbf{H}_a^T\mathbf{P} \tag{37}$$

Finally, (15) can be transferred into the LMIs (29) and (30) by applying the lemma given in (Peterson and Hollot, 1986) and the Schur complement. The LMIs (29) and (30) are solved numerically and will be used as constraints in the optimization problem solved by GWO in the next section.

5. OPTIMAL TUNING OF TAKAGI-SUGENO PI-FUZZY CONTROLLERS USING GWO

The design of the Takagi-Sugeno PI-fuzzy controller included the parameter tuning, i.e. obtain the values of the parameters in the constant state feedback matrices $\mathbf{k}_i = [k_{i\omega\eta}]_{\omega=1\ldots n+1,\eta=1\ldots m} \in R^{(n+1)\times m}$. The gains of these matrices are grouped in the parameter vector $\boldsymbol{\rho}$. The membership functions are fixed and only the gains are optimized.

The constrained optimization problem that ensures the stable design of the Takagi-Sugeno PI-fuzzy controllers is defined as follows:

$$\boldsymbol{\rho}^{*}=\arg\min_{\boldsymbol{\rho}} J(\boldsymbol{\rho}), J(\boldsymbol{\rho})=\int_{0}^{t_f} e^{2}(t)dt \text{ s.t.}(29),(30) \tag{38}$$

where $\boldsymbol{\rho}^{*}$ is the optimal value of the vector $\boldsymbol{\rho}$, e is the control error, $J(\boldsymbol{\rho})$ is the objective function and $[0,t_f]$ is the time horizon. As pointed out in Section 1, the optimization problem (38) is solved in this paper by GWO, which is next briefly described.

As shown in (Precup et al., 2017a), (Precup et al., 2017b), the operating mechanism of GWO starts with the random initialization of the agents that comprise the wolf pack. A total number of *N* agents (grey wolves) is used, and each agent is assigned to a position vector $\mathbf{X}_i(k)$:

$$\mathbf{X}_i(k)=[x_i^1(k) \quad ... \quad x_i^f(k) \quad ... \quad x_i^q(k)]^T, i=1...N \tag{39}$$

where $x_i^f(k)$ is the position of i^{th} agent in the f^{th} dimension, $f=1...q$, *k* is the index of the current iteration, $k=1...k_{\max}$, and $k_{\max}$ is the maximum number of iterations.

The operating mechanism (the search process of it) continues with the exploration stage, where the positions of the top three agents, namely the alpha (α), beta (β), and delta (δ) agents, dictate the search pattern by diverging from other agents and converging to the prey (the solution to (38)).

The exploitation stage models the attack on the prey, where the top three agents force the remaining agents (the omega (ω) ones) to update their positions according to theirs. The following notations are used for the top three agent position vectors (Precup et al., 2017b):

$$\mathbf{X}^l(k)=[x^{l1}(k) \quad ... \quad x^{lf}(k) \quad ... \quad x^{lq}(k)]^T, l\in\{\alpha,\beta,\delta\} \tag{40}$$

The top three vector solutions $\mathbf{X}^{\alpha}(k)$, $\mathbf{X}^{\beta}(k)$ and $\mathbf{X}^{\delta}(k)$, are obtained in a three-step selection process:

$$\begin{aligned}
&J(\mathbf{X}^{\alpha}(k))=\min_{i=1...N}\{J(\mathbf{X}_i(k))\,|\,\mathbf{X}_i(k)\in D_{\boldsymbol{\rho}}\}\\
&J(\mathbf{X}^{\beta}(k))=\min_{i=1...N}\{J(\mathbf{X}_i(k))\,|\,\mathbf{X}_i(k)\in D_{\boldsymbol{\rho}}\setminus\{\mathbf{X}^{\alpha}(k)\}\}\\
&J(\mathbf{X}^{\delta}(k))=\min_{i=1...N}\{J(\mathbf{X}_i(k))\,|\,\mathbf{X}_i(k)\in D_{\boldsymbol{\rho}}\setminus\{\mathbf{X}^{\alpha}(k),\mathbf{X}^{\beta}(k)\}\}\\
&J(\mathbf{X}^{\alpha}(k))<J(\mathbf{X}^{\beta}(k))<J(\mathbf{X}^{\delta}(k))
\end{aligned} \tag{41}$$

The *a* and *c* coefficients are then defined:

$$a_l^f(k)=a^f(k)(2r_{1l}^f-1), c_l^f(k)=2r_{2l}^f, l\in\{\alpha,\beta,\delta\} \tag{42}$$

where r_{1l}^f and r_{2l}^f are uniformly distributed random numbers, $0\le r_{1l}^f\le 1$, $0\le r_{2l}^f\le 1$, $f=1...q$, and the coefficients $a^f(k)$ are linearly decreased from 2 to 0 during the search process:

$$a^f(k) = 2(1 - \frac{k-1}{k_{\max}-1}),\ f = 1...q \tag{43}$$

The approximate distances between the current solution and the alpha, beta, and delta solutions (with the notations $d_{\alpha}^{if}(k)$, $d_{\beta}^{if}(k)$ and $d_{\delta}^{if}(k)$ according to (Precup et al., 2017b)) are:

$$d_{\alpha}^{if}(k) = |c_i^f(k)x^{lf}(k) - x_i^f(k)|,\ i = 1...N,\ f = 1...q,\ l = \alpha \tag{44}$$

$$d_{\beta}^{if}(k) = |c_i^f(k)x^{lf}(k) - x_i^f(k)|,\ i = 1...N,\ f = 1...q,\ l = \beta$$

$$d_{\delta}^{if}(k) = |c_i^f(k)x^{lf}(k) - x_i^f(k)|,\ i = 1...N,\ f = 1...q,\ l = \delta$$

The components of the updated alpha, beta, and delta solutions are next obtained as:

$$x^{lf}(k+1) = x^{lf}(k) - a_l^f(k)d_l^{if}(k),\ f = 1...q, i = 1...N, l \in \{\alpha, \beta, \delta\} \tag{45}$$

and they lead to the update law for agents' positions:

$$x_i^f(k+1) = [x^{\alpha f}(k+1) + x^{\beta f}(k+1) + x^{\delta f}(k+1)]/3,\ f = 1...q, i = 1...N \tag{46}$$

also expressed in vector form as:

$$\mathbf{X}_i(k+1) = [\mathbf{X}^{\alpha}(k+1) + \mathbf{X}^{\beta}(k+1) + \mathbf{X}^{\delta}(k+1)]/3, i = 1...N \tag{47}$$

The GWO algorithm is mapped onto the optimization problems using:

$$\mathbf{X}_i(k) = \boldsymbol{\rho}, i = 1...N, \boldsymbol{\rho}^* = \arg\min_{i=1...N} J(\mathbf{X}_i(k_{\max})) \tag{48}$$

5. SIMULATION RESULTS

The model-free sliding mode controller and the Takagi-Sugeno fuzzy controller are tested as follows using the RODP process model presented in Section 2 and the controller designs presented in sections 3 and 4. Simulation results are given and not all details on the parameters are offered because of certain constraints.

The two control loops are tested by considering four controllers in each of them: a model-free sliding mode controller (MFSMC), a Takagi-Sugeno PI-fuzzy controller (TSPIFC) proposed in this paper, a PI fuzzy controller optimized by GWO (PICGWO), and a PI fuzzy controller optimized by GSA (PICGSA) using a GSA implementation applied from (Purcaru et al., 2013) and (Vrkalovic et al., 2017). The last two controllers are used for comparison. In order to offer a fair comparison, although one controller is tuned in a model-free manner and three controllers are tuned in a model-based manner, the optimal tuning of all controllers is carried out in a model-based manner by solving the optimization problems of type (38) for both control loops.

The closed-loop responses observed for the controllers applied to the flux control loop are presented in Figure 3. The closed-loop responses obtained for the control systems with controllers applied to the conductivity control loop are presented in Figure 4. The simulation results show that the best controller for the flux loop is the model-free sliding mode controller, and the best one for the conductivity loop is the fuzzy controller.

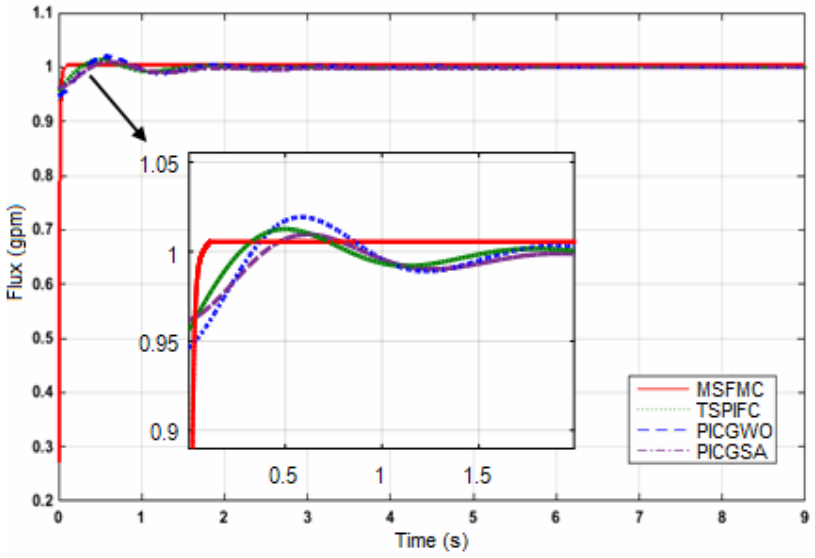

Figure 3. Controlled output step response for flux control loop.

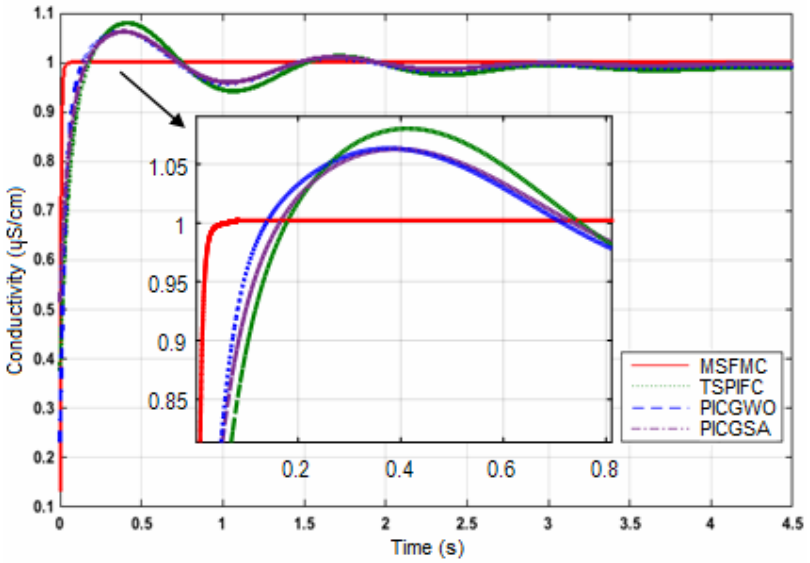

Figure 4. Controlled output step response for conductivity control loop.

6. CONCLUSIONS

The paper has presented the design of a model-free sliding mode controller and a Takagi-Sugeno PI-fuzzy controller for RODP. Some simulation results have been given. The stability analysis and the optimization have been used in the tuning of the fuzzy controller. But, for a fair comparison, the model-based optimal tuning has been applied to tune the free parameters of all controllers, model-based and model-free ones. However, the model-free versus model-based tuning remains an open issue although the performance of the control systems presented in this paper is similar.

The presentation of these controllers is sufficiently general to be used to other processes. Future research will deal with different processes and different controllers as well including PID ones and other controller structures.

REFERENCES

Alatiqi, I.M., Ghabris, A.H., Ebrahim, S., 1989, System identification and control of reverse osmosis desalination. *Desalination* **75**, 119–140.

Castillo, O., Neyoy, H., Soria, J., Melin, P., Valdez, F., 2015, A new approach for dynamic fuzzy logic parameter tuning in ant colony optimization and its application in fuzzy control of a mobile robot. *Applied Soft Computing* **28**, 150-159.

Chaaben, A.B., Andoulsi, R., Sellami, A., Mhiri, R., 2011, MIMO modeling approach for a small photovoltaic reverse osmosis desalination system. *Journal of Applied Fluid Mechanics* **4**, 35–41.

Chang, X.-H., Park, J.H., Shi, P., 2017, Fuzzy resilient energy-to-peak filtering for continuous-time nonlinear systems. *IEEE Transactions on Fuzzy Systems* **25**, 6, 1576–1588.

Das, S., Pan, I., Das, S., 2013, Fractional order fuzzy control of nuclear reactor power with thermal-hydraulic effects in the presence of random network induced delay and sensor noise having long range dependence. *Energy Conversion and Management* **68**, 200–218.

Du, Z.-B., Lin, T.-C., Song, P., Lin, Y.-C., 2017, Fuzzy mixed H_2/H_∞ sampled-data control design for nonlinear dynamic systems. *Control Engineering and Applied Informatics* **19**, 3, 13–21.

Gambier, A., Krasnik, A., Badreddin, E., 2007, Dynamic modeling of a simple reverse osmosis desalination plant for advanced control purposes. *Proceedings of 2007 American Control Conference*, New York, NY, USA, 4854–4859.

Gambier, A., Wellenreuther, A., Badreddin, E., 2009, Control system design of reverse osmosis plants by using advanced optimization techniques. *Desalination and Water Treatment* **10**, 1–3, 200–209.

Gao, L., Rahardianto, A., Gu, H., Christofides, P.D., Cohen, Y., 2014, Energy-optimal control of RO desalination. *Industrial & Engineering Chemistry Research* **53**, 18, 7409–7420.

Haidegger, T., Kovacs, L., Precup, R.-E., Benyo, B., Benyo, Z., Preitl, S., 2012, Simulation and control for telerobots in space medicine. *Acta Astronautica* **181**, 1, 390–402.

Kazakov, A.L., Lempert, A.A., 2015, On mathematical models for optimization problem of logistics infrastructure. *International Journal of Artificial Intelligence* **13**, 1, 200–210.

Khooban, M.-H., 2018, Secondary load frequency control of time-delay stand-alone microgrids with electric vehicles. *IEEE Transactions on Industrial Electronics* **65**, 9, 7416–7422.

Lee, S.-K., Myung, S.-H., Hong, J.-H., Har, D.-S., 2016, Reverse osmosis desalination process optimized for maximum permeate production with renewable energy. *Desalination* **398**, 133–143.

Li, H.-Y., Wang, J.-H., Wu, L.-G., Lam, H.-K., Gao, Y.-B., 2018, Optimal guaranteed cost sliding-mode control of interval type-2 fuzzy time-delay systems. *IEEE Transactions on Fuzzy Systems* **26**, 1, 246–257.

Melin, P., Astudillo, L., Castillo, O., Valdez, F., Garcia, M., 2013, Optimal design of type-2 and type-1 fuzzy tracking controllers for autonomous mobile robots under perturbed torques using a new chemical optimization paradigm. *Expert Systems with Applications* **40**, 3185–3195.

Perez, J., Milanés, V., Godoy, J., Villagrá, J., Onieva, E., 2013, Cooperative controllers for highways based on human experience. *Expert Systems with Applications* **40**, 1024–1033.

Peterson, I.R., Hollot, C.V., 1986, A Riccati equation approach to the stabilization of uncertain linear systems. *Automatica* **22**, 397–411.

Phuc, B.D.H., You, S.-S., Choi, H.-S., Jeong, S.-K., 2016, Advanced control synthesis for reverse osmosis water desalination processes. *Water Environment Research* **89**, 11, 1932–1941.

Pozna, C., Minculete, N., Precup, R.-E., Koczy, L.T., Ballagi, A., 2012, Signatures: Definitions, operators and applications to fuzzy modeling. *Fuzzy Sets and Systems* **201**, 86–104.

Precup, R.-E., Angelov, P., Costa, B.S.J., Sayed-Mouchaweh, M., 2015, An overview on fault diagnosis and nature-inspired optimal control of industrial process applications. *Computers in Industry* **74**, 75–94.

Precup, R.-E., David, R.-C., Petriu, E.M., 2017a, Grey wolf optimizer algorithm-based tuning of fuzzy control systems with reduced parametric sensitivity. *IEEE Transactions on Industrial Electronics* **6**4, 1, 527–534.

Precup, R.-E., David, R.-C., Szedlak-Stinean, A.-I., Petriu E.M., Dragan, F., 2017b, An easily understandable grey wolf optimizer and its application to fuzzy controller tuning. *Algorithms* **10**, 2, paper 68, 1–15.

Precup, R.-E., Preitl, S., Petriu, E.M., Tar, J.K., Tomescu, M.L., Pozna, C., 2009, Generic two-degree-of-freedom linear and fuzzy controllers for integral processes. *Journal of the Franklin Institute* **346**, 10, 980–1003.

Precup, R.-E., Radac, M.-B., Petriu, E.M., Dragos, C.-A., Preitl, S., 2014, Model-free tuning solution for sliding mode control of servo systems. *Proceedings of 8th Annual IEEE International Systems Conference*, Ottawa, ON, Canada, pp. 30–35.

Precup, R.-E., Radac, M.-B., Roman, R.-C., Petriu, E.M., 2017c, Model-free sliding mode control of nonlinear systems: algorithms and experiments. *Information Sciences* **381**, 176–192.

Precup, R.-E., Radac, M.-B., Tomescu, M.L., Petriu, E.M., Preitl, S., 2013, Stable and convergent iterative feedback tuning of fuzzy controllers for discrete-time SISO systems. *Expert Systems with Applications* **40**, 1, 188–199.

Preitl, S., Precup, R.-E., Fodor, J., Bede, B., 2006, Iterative feedback tuning in fuzzy control systems. Theory and applications. *Acta Polytechnica Hungarica* **3**, 3, 81–96.

Purcaru, C., Precup, R.-E., Iercan, D., Fedorovici, L.-O., David, R.-C., Dragan, F., 2013, Optimal robot path planning using gravitational search algorithm. *International Journal of Artificial Intelligence* **10**, S13, 1–20.

Rathinasamy, S., Rathika, M., Kaviarasan, B., Shen, H., 2018, Stabilization criteria for singular fuzzy systems with random delay and mixed actuator failures. *Asian Journal of Control* **20**, 2, 829–838.

Rathore, N.S., Kundariya, N., Narain, A., 2013, PID controller tuning in reverse osmosis system based on particle swarm optimization. *International Journal of Scientific and Research Publications* **3**, 6, 1–5.

Rathore, N.S., Singh, P., 2018a, Design of optimal PID controller for the reverse osmosis using teacher-learner-based-optimization. *Membrane Water Treatment* **9**, 2, 129–136.

Rathore, N.S., Singh, P., Bhavnesh, K., 2018b, Controller design for Doha water treatment plant using grey wolf optimization. *Journal of Intelligent & Fuzzy Systems* **DOI: 10.3233/JIFS-169815**, 1–8.

Riverol, C., Pilipovik, V., 2005, Mathematical modeling of perfect decoupled control system and its application: A reverse osmosis desalination industrial-scale unit. *Journal of Analytical Methods in Chemistry* **2005**, 2, 50–54.

Robertson, M.W., Watters, J.C., Desphande, P.B., Assef, J.Z., Alatiqi, I.M., 1996, Model based control for reverse osmosis desalination processes. *Desalination* **104**, 59–68.

Škrjanc, I., Blažič, S., Matko D., 2002, Direct fuzzy model-reference adaptive control. *International Journal of Intelligent Systems* **17**, 10, 943–963.

Tomescu, M.L., Preitl, S., Precup, R.-E., Tar, J.K., 2007, Stability analysis method for fuzzy control systems dedicated controlling nonlinear processes. *Acta Polytechnica Hungarica* **4**, 3, 127–141.

Vrkalovic, S., 2015, An application of symmetrical optimum method to servo systems with variable inertia. *Gradus* **2**, 1, 191–199.

Vrkalovic, S., Teban, T.-A., Borlea, I.-D., 2017, Stable Takagi-Sugeno fuzzy control designed by optimization. *International Journal of Artificial Intelligence* **15**, 2, 17–29.

Wang, H.-P., Tian, Y., Han, S.-S., Wang, X.-K., 2017, ZMP theory-based gait planning and model-free trajectory tracking control of lower limb carrying exoskeleton system. *Studies in Informatics and Control* **26**, 2, 161–170.

Wang, H.-P., Ye, X.-F., Tian, Y., Christov, N, 2015, Attitude control of a quadrotor using model free based sliding model controller. *Proceedings of 2015 20th International Conference on Control Systems and Science*, Bucharest, Romania, 149–154.

Wang, L., Yang, R., Pardalos, P.M., Qian, L., Fei, M., 2013, An adaptive fuzzy controller based on harmony search and its application to power plant control. *International Journal of Electrical Power and Energy Systems* **53**, 272–278.

Wang, X., Li, X., Wang, J., Fang, X., Zhu, X., 2016, Data-driven model-free adaptive sliding mode control for the multi degree-of-freedom robotic exoskeleton. *Information Sciences* **327**, 246–257.